Ultrasonic Thickness Estimation using Multimodal Guided Lamb Waves generated by EMAT

Joaquín García-Gómez[1], Roberto Gil-Pita[1], Antonio Romero-Camacho[2], Jesús Antonio Jiménez-Garrido[2], Víctor García-Benavides[2], César Clares-Crespo[1], Miguel Aguilar-Ortega[1]

[1] Signal Theory and Communications Department
University of Alcala
Alcala de Henares, Madrid, Spain
(34) 91-8856751; fax (34) 91-8856699; email roberto.gil@uah.es

[2] Innerspec Technologies Europe S.L
Torres de la Alameda, Madrid, Spain

ABSTRACT

The objective of this paper is to study how the selection of the coil and the frequency affects the received modes in guided Lamb waves, with the objective of analyzing the best configuration for determining the depth of a given defect in a metallic pipe with the minimum error. Studies of the size of the damages with all the extracted parameters are then used to propose estimators of the residual thickness, considering amplitude and phase information in one or several modes. Results demonstrate the suitability of the proposal, improving the estimation of the residual thickness when two simultaneous modes are used, as well as the range of possibilities that the coil and frequency selection offers.

Keywords: EMAT sensors, Lamb waves, pipeline inspection, defect sizing, coil selection, frequency selection

INTRODUCTION

Defect sizing in pipeline inspection allows companies to determine when a pipe must be replaced, avoiding costly repairs in their assets. To tackle this issue, Lamb ultrasonic waves generated through Electro-Magnetic Acoustic Transducers (EMAT) allow thickness estimation without direct contact with the surface of the metallic material under investigation [1]. The use of this technology with a meander-line-coil allows generating waves in a directional way [2], which facilitates differentiating between circumferential and axial scans in Non-Destructive Testing (NDT) for pipeline inspection [3].

However, the shape of the defect changes the behavior of the ultrasonic signals when they pass through the pipeline, and it is not easy to predict the amplitude and phase of the wave in function of the residual thickness [4,5]. In recent studies the use of machine learning techniques applied to information extracted from signals sensed at different frequencies has been demonstrated to improve the accuracy of the estimation, but the use of multiple frequencies in general requires more complex sensing devices and more time. A possible way to address these disadvantages is the use of different modes sensed at a unique frequency, but in this case the selection of the coil and the inspection frequency becomes a critical aspect, since these different modes must be separable in the measurement, and this is not always the case.

This paper presents a theoretical study in which the selection of the coil and the frequency for multimodal thickness estimation are analyzed. The objective is to determine the relationship between the performance of the estimator and the configuration of the sensing system. The problem was approached from two perspectives. First, a signal processing based theoretical framework is proposed. Second, simulations obtained by a Finite Element software are considered. Results demonstrate the suitability of the proposals, improving the estimation of the residual thickness.

LAMB WAVE GENERATION USING EMAT SENSORS

In this section the generation of Lamb waves through EMAT sensors will be described. These sensors are composed of a magnet and a coil wire. The current is induced in the surface of the ferromagnetic material when the alternating electrical current flow through the coil wire is placed in a uniform magnetic field near the material. When this field interacts with the field generated by the magnet, Lorentz force appears. Because of that, a disturbance affects to the material, creating an elastic wave. If the vibration is coplanar with the propagation plane, these waves are called Lamb waves. Conversely, the interaction of Lamb waves with a magnetic field induces current in the EMAT receiver coil circuit.

Lamb waves are characterized by their dispersion and sensitivity to thickness variations. Besides, they can be divided into modes: symmetric and asymmetric modes. Each mode is composed of two waves (longitudinal and transversal). They travel at different angles θ_L and θ_T with velocities c_L and c_T, where the latter refer to the sound velocity in longitudinal and transversal components, respectively. Considering a Lamb mode that moves in the x direction at velocity c_p with a frequency f, then the wavenumber k is related to the longitudinal and transversal components of the wave:

$$k_L \cos\theta_L = k_T \cos\theta_T = k = \frac{2\pi f}{c_p} \quad \textbf{(Eq. 1)}$$

where $k_L = 2\pi f / c_L$ and $k_T = 2\pi f / c_T$, are the wavenumber of the longitudinal and transversal components, respectively. Furthermore, the displacement of each wave in the z axis can be obtained using α_L and α_T, so that:

$$\alpha_L = k_L \sin\theta_L = 2\pi f \sqrt{\frac{1}{c_L^2} - \frac{1}{c_p^2}} \quad \textbf{(Eq. 2)}$$

$$\alpha_T = k_T \sin\theta_T = 2\pi f \sqrt{\frac{1}{c_T^2} - \frac{1}{c_p^2}} \quad \textbf{(Eq. 3)}$$

Considering that the wave is reflected in the surfaces and applying the boundary conditions, we can get an equation related to the dispersion of the Lamb modes. Equation (4) refers to the symmetric modes and equation (5) refers to asymmetric ones.

$$4k^2\alpha_L\alpha_T \sin\left(\frac{\alpha_L h}{2}\right)\cos\left(\frac{\alpha_T h}{2}\right) + \sin\left(\frac{\alpha_T h}{2}\right)\cos\left(\frac{\alpha_L h}{2}\right)(\alpha_T^2 - k^2)^2 = 0 \quad \textbf{(Eq. 4)}$$

$$4k^2\alpha_L\alpha_T \cos\left(\frac{\alpha_L h}{2}\right)\sin\left(\frac{\alpha_T h}{2}\right) + \cos\left(\frac{\alpha_T h}{2}\right)\sin\left(\frac{\alpha_L h}{2}\right)(\alpha_T^2 - k^2)^2 = 0 \quad \textbf{(Eq. 5)}$$

From the previous equations, it can be derived that there exists a relation between the excited frequency f, the thickness of the pipe h and the phase velocity c_p. In particular, each mode travels at different c_p depending on the other above-mentioned parameters. We get a similar relation with the group velocity c_g, defined in equation (6).

$$c_g = c_p^2 \left(c_p - fh\frac{\partial c_p}{\partial fh}\right)^{-1} \quad \textbf{(Eq. 6)}$$

Solving the previous equations for different values of frequency and thickness we obtain the phase and group velocity for each propagating mode.

Now we will consider how signals are generated and received in the pipeline. The EMAT system consists of a meander-line-coil which generates two signals per loop in the system (one per meander). These waves are characterized by their wavelength which depends on the separation of the meanders. The following equations are valid for one mode and then we will iterate for all the modes which appear at a given frequency. Thus, we have to set the wave equation depending on the group and phase velocities. Considering f as the excited frequency, the transmitted signal propagating in the x axis will be generated according to equation (7).

$$s(x,t) = \sin\left(2\pi f\left(t - \frac{x}{c_p}\right)\right) \quad \textbf{(Eq. 7)}$$

Please note here that the velocity c_p will depend on the frequency and the thickness of the pipe. In a real case, the transmitted signal includes an envelope $w(t)$ that generates the transmitted wave packet $p(x,t)$. This envelope limits the transmission time, and allows controlling the length of the transmitted pulse. Typically, the length of this envelope is described in function of C, the number of cycles included in the wave packet. This envelope will travel at an average velocity of c_g, and in general its shape will change with the distance due to dispersion effects. So, once the envelope is considered, the transmitted wave packet $p(x,t)$ will be expressed using equation (8).

$$p(x,t) = \sin\left(2\pi f\left(t - \frac{x}{c_p}\right)\right)\widehat{w}\left(t - \frac{x}{c_g}\right) \quad \textbf{(Eq. 8)}$$

From this point, instead of using the transmitted envelope $w(t)$ we will use using $\widehat{w}(t)$, which changes its shape in function of the distance due to dispersion effects. It is also necessary to consider that under EMAT technology the excitation signal is generated in a set of N loops of a coil, separated by a distance L, which will generate the propagation wave $y(x,t)$ using equation (9).

$$y(x,t) = \sum_{m=1}^{2N}(-1)^m \sin\left(2\pi f\left(t - \frac{x + m\frac{L}{2}}{c_p}\right)\right)\widehat{w}\left(t - \frac{x + m\frac{L}{2}}{c_g}\right) \quad \textbf{(Eq. 9)}$$

Each loop generates two signals (one per meander), and the sign of their contribution to the propagation wave $y(x,t)$ is included in the term $(-1)^m$. Besides, the measure is sensed at a distance D, in another set of N loops separated by a distance L. So, the received signal $z(t)$ will be expressed using equation (10).

$$z(t) = \sum_{n=1}^{2N}\sum_{m=1}^{2N}(-1)^{m+n} \sin\left(2\pi f\left(t - \frac{x + (m+n)\frac{L}{2}}{c_p}\right)\right)\widehat{w}\left(t - \frac{x + (m+n)\frac{L}{2}}{c_g}\right) \quad \textbf{(Eq. 10)}$$

The signal received from each mode $z(t)$ has different values of c_p and c_g, as it was concluded from equations (4), (5) and (6). Thus, each mode arrives at the receiver with different amplitude and envelope, depending on the attenuation of each mode and the difference of phase when the signal is received in the coil. Therefore, the amount of energy of the received signal will vary in function of the frequency.

In order to find out more about the behavior of the modes, a frequency sweep has been carried out between 0 and 800 kHz with one coil and $C = 4$ cycles per wave packet. Figure 1 shows the phase velocity (left) and group velocity (right), where black color means the energy is maximum at that frequency. Dispersion has been taken into account to carry out these experiments, since the signal $p(x,t)$ has been decomposed with the envelope window

$\widehat{w}(t)$ through the Fourier Transform, and different velocity has been applied to each frequency component. These graphs correspond to a steel pipe with the following parameters: Young's modulus $E = 210 \cdot 10^9\, N/m^2$, Poisson's ratio $\nu = 0.3$ and density $\rho = 7800\ kg/m^3$.

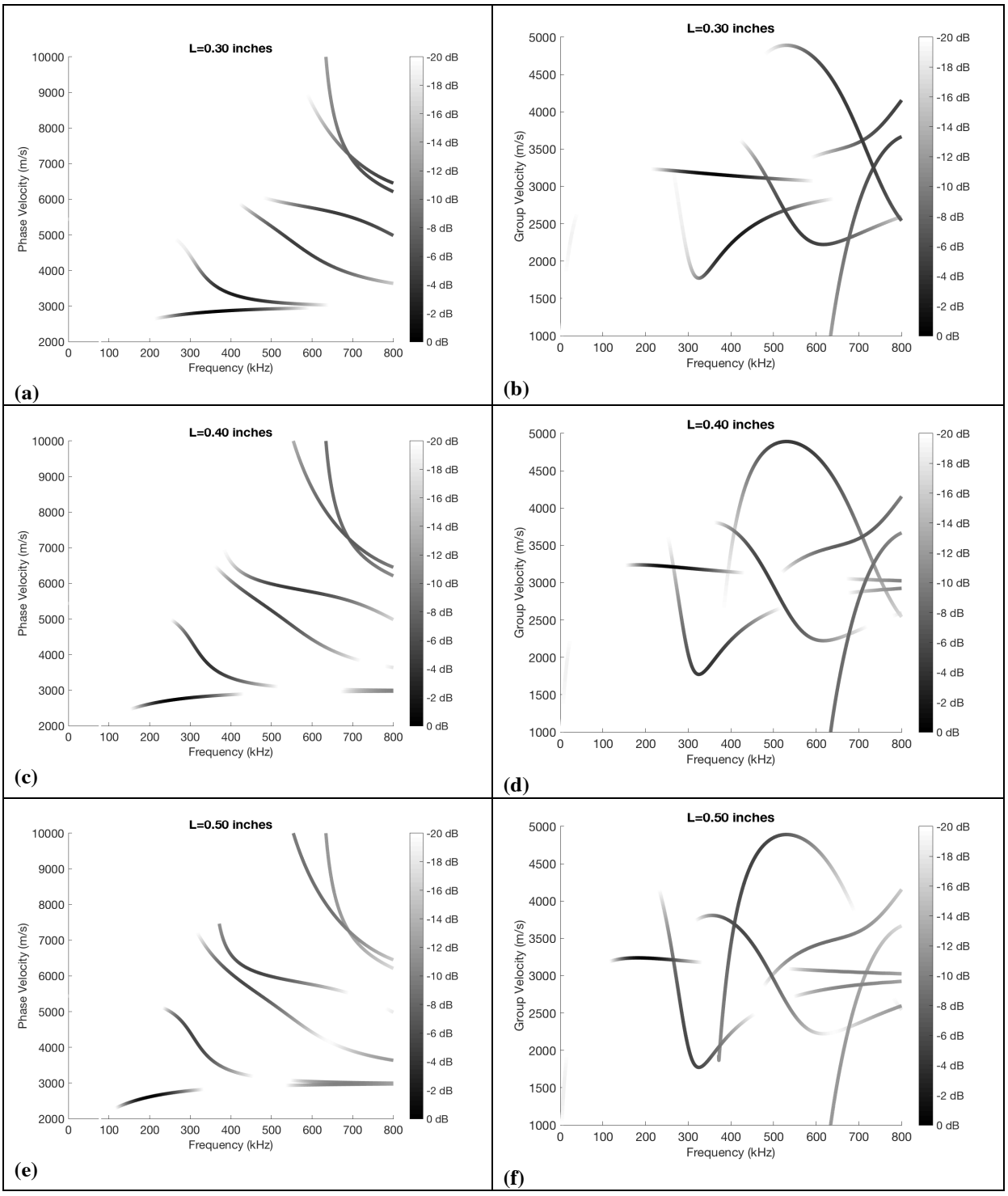

Figure 1: Phase velocity (a) and group velocity (b) in function of the product frequency by thickness, using coils with different *L* value.

The coil used in the experiments has the following parameters: distance between loops L ranging from 0.3 to 0.5 inches, and $N = 3$ loops. It can be observed that the same coil could be used to excite other frequencies, even if it has been designed to get the maximum energy in a given frequency. Furthermore, if we want to analyze the behavior of the modes in a deep way, we could change the length L of the coil. In Figure 1 it is observed that the points and areas of maximum energy vary significantly from one coil to another.

FREQUENCY AND COIL SELECTION FOR MULTIMODAL FEATURE EXTRACTION

The modeling of the pipeline by means of the ultrasound waves is a non-trivial problem. The changing shape of the defects makes difficult to draw general conclusions about the relation between the defect and the received signals. The distortion caused by the defects over the different modes strongly varies with the shape of the mode [4,5]. For instance, the amplitude of the signal, the time of arrival (group velocity c_g) and the phase velocity c_p of the wrap-around signal vary with the dimension and shape of the defect.

Thus, it is necessary to analyze how the different modes are going to be represented in the received signal, in order to look for the best configuration (frequency and size of the coil) that allows a better representation of the different modes over the same signal.

As it was stated, a meander-line-coil is used to generate the ultrasonic signals that are analyzed once they wrap the pipeline. It allows us to know the condition of the pipes depending on the different modes and wrap arounds received. In order to investigate how the behavior of the modes changes according to the length of the coil, a sweep of experiments has been carried out with coils from 0.30 inches to 0.55 inches, in steps of 0.01 inches. The most relevant results are shown in Figure 2, where we show where the energy of the different modes is located in a time-frequency representation. Both asymmetric (A0, A1, A2, A3) and symmetric (S0, S1, S2, S3) modes are plot in different colors. In each of the modes, curves indicate the area where the energy of the mode is higher or lower.

Results from this figure show that as we change the length of the coil, the parameters related to the modes (frequency of appearance, area of maximum energy, etc.) are not the same. The final effect is that the modes “move” in frequency and time. For instance, as the length of the coil in higher, some of the modes appear at lower frequencies. That is the case of A0, S0, A1 and S1 modes. Other modes disappear from the observed window, such as the A2 mode (pink), whose second wrap around went away from 0.40 inches to 0.45 inches. First wrap around disappear from 0.45 inches to 0.50 inches.

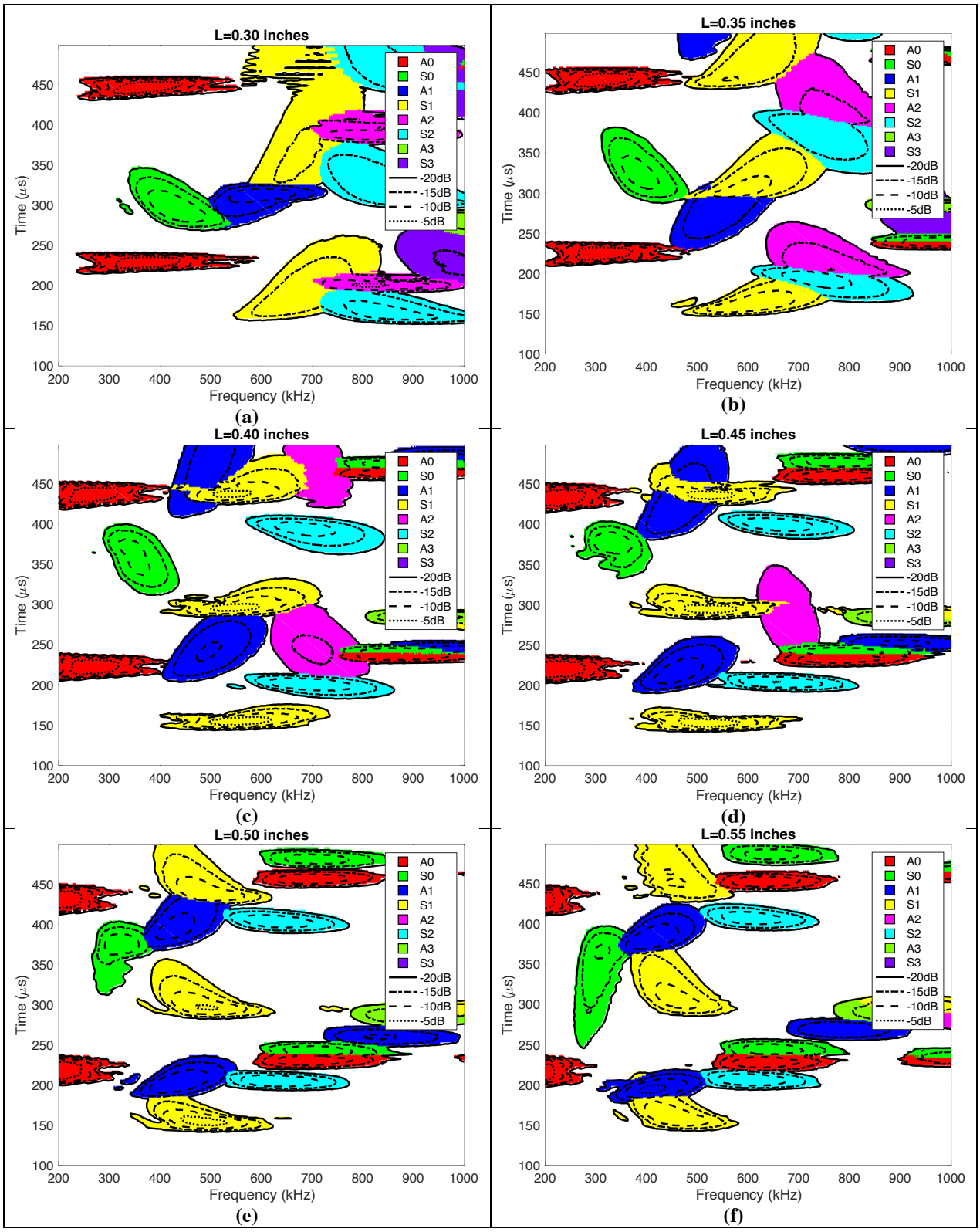

Figure 2: Energy localization of the different modes in function of the frequency.

However, the usefulness of these graphs is that we can set a frequency depending on the modes or wrap arounds we are interested in, particularly when the objective is not to use just one mode. For instance, if we want to focus on modes A1 and S1 (dark blue and yellow), it can be seen that 0.30 and 0.35 inches are not the suitable lengths because both modes will appear mixed in the received signal. We should choose a higher value, such as 0.45 inches, where first wrap-around of A1 mode as well as first and second wrap around from S1 mode are well separated in time between 400 and 600 kHz approximately, so they will not be overlapped. Other option would be to choose a value of 0.50 inches, where these modes are almost completely separated, but including the second wrap-around of both modes or even the third one from the S1 mode. Again, it is clear that 0.55 inches is not a suitable value because these modes start to appear together again.

SMART SOUND PROCESSING FOR SIZING ESTIMATION

If we want to solve the problem of pipeline sizing, it is necessary to apply a pattern recognition system, which is composed of two stages. In the first stage, useful information is extracted from the signals in the form of features. Later, in a second stage, a predictor tries to learn a model which will be useful for predicting the defects presented in the pipeline.

To extract useful information from the received signal is very important in the process, since it will be the "raw material" that the predictor will use. Analyzing a set of signals from real pipelines and the state of the art [6], we observe that the following features could be useful for the problem at hand:

- Average echo energy (dB), which represents the average energy of the echo received.
- Peak wrap-around energy (dB), which represents the maximum energy of the pulse. We have considered ± 30 μs around t_0, the maximum of the signal in the case of absence of defect, to look for the maximum of each signal.
- Average wrap-around energy (dB), which represents the average energy of the pulse. We have considered ± 30 μs around t_0, the maximum of the signal in the case of absence of defect.
- Wrap-around phase delay (μs), which represents how much time has passed between the pulse was sent and it was received in the same point of the pipeline. It is determined measuring the time difference between t_0 and its closest maximum in $z(t)$. Please note that a delay larger than $1/2f$ causes uncertainty, which conditions the usefulness of this measurement.
- Wrap-around group delay (μs), denoted $\widehat{t_g}$. In order to estimate this measurement, we consider the centroid of the average energy of the pulse around t_0, with equation (11).

$$\widehat{t_g} = \frac{\sum_{t=t_0-3\cdot10^{-5}}^{t_0+3\cdot10^{-5}} t\, z(t)^2}{\sum_{t=t_0-3\cdot10^{-5}}^{t_0+3\cdot10^{-5}} z(t)^2} \qquad \textbf{(Eq. 11)}$$

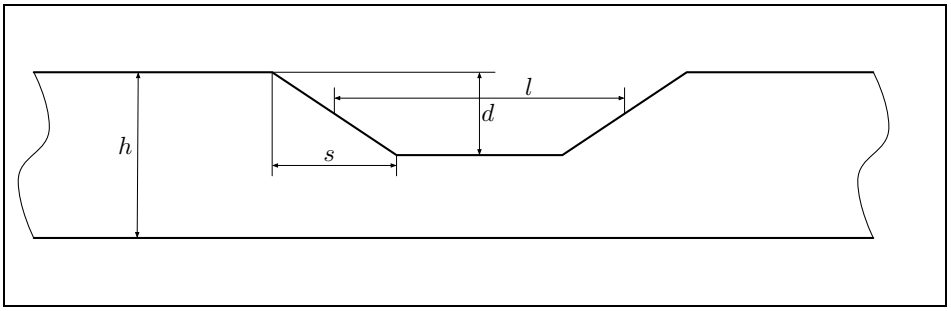

Figure 3: Model of the simulated defects.

Once we have obtained the features, we need to apply a nonlinear predictor to get the final profile of the pipeline and to know the performance of the developed model. Neural Networks have been applied, specifically the Multi Layer Perceptron (MLP) [7]. In this paper MLPs with a hidden layer of twenty neurons have been trained using the Levenberg-Marquardt algorithm [8].

From the results presented in Figure 2, we will select and $f = 450$ and a coil with $L = 0.52$ inches. So, in the case of using just the main mode we will consider 5 features, and in the case of considering two modes we will have 9 features (4 wrap-around features for each mode plus the echo energy).

To study the relationship between these parameters and the shape of the defects, we have used the Finite Element Method (FEM) included in the Partial Differential Equations Toolbox of *Matlab*. With these simulations we have generated a database with several different defects. The defects have been characterized with three parameters: length (l), depth (d) and slope (s). Figure 3 describes the meaning of these parameters in a real pipeline. The thickness of the pipe used is $h = 7.8$ mm, and the distance to the receiver is $D = 0.7$ m. For simplicity, we have not modeled the width of the defect, that is to say, we have not considered the y dimension of the pipeline.

Table 1: RMSE (mm) in the estimation of the residual thickness using an MLP with 20 neurons in the hidden layer for different number of used modes.

	S1 mode 5 features	**S1 and A1 modes 9 features**
RMSE (mm)	10.50 mm	9.72 mm

In a second approach, we have developed an experiment using a synthetic database for estimating the residual thickness of the pipeline. The database consists of 384 signals generated with defects of different shape. The length of the defect (l) ranged from 10 to 100 mm, the depth (d) from 0 to 9 mm, and the slope (s) from 1 to 100 mm.

To obtain the prediction results, k-fold cross validation was applied in the generated database, being $k = 5$. This method consists in dividing the database in k groups so that the full process is repeated k times, using one group of signals as test subset and the remaining $k - 1$ groups as training subset. Results are then averaged to obtain the Root Mean Square Error (RMSE) of the estimation of the depth. The advantage of this method is that the obtained results are generalizable to defects different from those used in the database.

The objective is to know how well estimated is the received signal at different frequencies, so different experiments have been considered. First, we have considered the use of only one frequency, and we have also studied what happens when both frequencies are used at the same time. Concerning the features, the usefulness of each feature has been studied, and the inclusion of all three features has also been considered. Table 1 shows the RMSE in function of the features and the frequencies. In all the cases above it is clear that as we get better results when two modes are used.

CONCLUSIONS

Pipeline inspection problem can be approached in many different ways. Lamb wave generation through EMAT sensors proves to be a very effective and useful one. However, the amount of information provided by the wrap-around signals needs to be processed by advanced techniques, such as smart sound processing algorithms. Thanks to them, it is feasible to get good estimation results of the pipeline defects, in both real and simulated signals.

In this paper we establish tools for determining the frequency and dimensions of the coil in order to be able to analyze two modes with an unique scan. We study how the behavior of the modes change when the length of the used coil is different, demonstrating its interest for multimodal approaches. Studies of the size of the damages with all the extracted parameters have been used to propose estimators of the residual thickness, considering amplitude and phase information. Results with two modes demonstrate the suitability of the proposal, improving the estimation of the residual thickness.

ACKNOWLEDGEMENTS

This work has been funded by Innerspec Technologies Europe S.L through the "Chair of modeling and processing of ultrasonic signals" (CATEDRA2007-001), and by the Spanish Ministry of Economy and Competitiveness-FEDER under Project TEC2015- 67387-C4-4-R.

CONFLICTS OF INTEREST

The authors declare that there is no conflict of interest

REFERENCES

(1) Green, R.E., 2004. "Non-contact ultrasonic techniques". *Ultrasonics*, 42, 9–16.

(2) Zhai, G., Jiang, T., Kang, L., 2014. "Analysis of multiple wavelengths of Lamb waves generated by meander-line coil EMATs". *Ultrasonics*, 54, 632–636.

(3) Salzburger, H.J., Niese, F., Dobmann, G., 2012. "EMAT pipe inspection with guided waves". *Welding in the world*, 56, 35–43.

(4) Demma, A., 2003. *The interaction of guided waves with discontinuities in structures. PhD thesis*, University of London.

(5) Cobb, A.C., Fisher, J.L., 2016. "Flaw depth sizing using guided waves". *AIP Conference Proceedings*. AIP Publishing, Vol. 1706, p. 030013.

(6) García-Gómez, J., Bautista-Durán, M., Gil-Pita, R., Romero-Camacho, A., Jimenez-Garrido, J.A., Garcia-Benavides,V., 2018, "Smart Sound Processing for Residual Thickness Estimation using Guided Lamb Waves generated by EMAT". *27th ASNT Research Symposium*, 99-105.

(7) Weisz, L., 2016. "Pattern Recognition Statistical Structural And Neural Approaches". *Pattern Recognition*, *1*, 2.

(8) Hagan, M.T.; Menhaj, M.B., 1994. "Training feedforward networks with the Marquardt algorithm". *IEEE transactions on Neural Networks*, *5*, 989–993.